Adsorption 3, 251–265 (1997)

Adsorption of Normal and Branched Paraffins in Faujasite Zeolites NaY, HY, Pt/NaY and USY

JOERI F.M. DENAYER AND GINO V. BARON
Department of Chemical Engineering, Vrije Universiteit Brussel, Pleinlaan 2, B-1050 Brussel, Belgium
jdenayer@vnet3.vub.ac.be
gvbaron@vnet3.vub.ac.be

Received July 16, 1996; Revised October 17, 1996; Accepted October 23, 1996

Abstract. The effect of chain length and branching of paraffins (from C6 to C12) on adsorption and diffusion in zeolites NaY, Pt/NaY, HY and USY has been investigated using the chromatographic method at 275–400°C. The Henry constants of the paraffins increase exponentially with the chain length (with a factor two per extra carbon group), the heats of adsorption increase with circa 7 kJ/mol per extra carbon group. Multicomponent sorption experiments reveal that longer chains are adsorbed preferentially over shorter chains, even at higher loadings. The multicomponent adsorption can be reasonably well described by an extended Langmuir adsorption isotherm, in which the stronger adsorption of the longer chains is reflected by their higher Henry constants. The molecular shape and zeolite type within this FAU group has only a small influence on the adsorption properties. Mass transfer in the pellets as used in catalytic conditions seems to be limited by macropore diffusion, rather than by micropore diffusion, which cannot be measured with the chromatographic method. Increasing the Si/Al-ratio of the zeolite reduces the adsorption capacity, but does not influence the relative adsorption properties.

Keywords: multicomponent equilibrium, zeolite, chromatography, paraffins, heat of adsorption

Introduction

Zeolite Y is undeniably a versatile catalyst in the field of catalytic cracking, hydrocracking and is used in a wide range of industrial processes. Due to its large pore size, this zeolite allows the reforming by isomerization of linear paraffins with a low octane number to branched, high octane isoparaffins (Bolton, 1976). Furthermore, the ultrastable form of this zeolite, USY, has the additional benefit of a reduced coke make, a long lifetime and a high hydrothermostability in comparison with other microporous catalysts (Ward, 1993). Despite the fact that most of the industrial hydrocarbon processes with Y zeolites are carried out with long chain hydrocarbons, only fragmentary information is available concerning the adsorption and diffusion of paraffins with carbon numbers above six in faujasites. Most of the papers deal with the diffusion and adsorption of C3–C7 paraffins and their isomers, cycloparaffins (Thamm et al., 1983; Harlfinger et al., 1983; Hrúzik et al., 1990; Atkinson and Curthoys, 1981), and finally aromatics (Hulme et al., 1991; Ruthven and Goddard, 1986; Eic et al., 1988; Moore et al., 1972; Satterfield et al., 1972; Ruthven and Goddard, 1986). Techniques like calorimetry, liquid and gas-solid chromatography and gravimetry are commonly used. The adsorption of normal paraffins from methane to *n*-decane on Na-X, Na-Y and Us-Ex was studied by Jänchen and Stach (Jänchen and Stach, 1985; Stach et al., 1986) using the isosteric method. The effect of molecular weight on the heat of adsorption for long chain normal paraffins (C4–C20 range) at 300–400°C in 5A en 13X was discussed by Burgess et al. (1964). Kärger et al. (1980) measured the self-diffusion of *n*-paraffins in zeolite NaX by means of the NMR pulsed field gradient technique, Eic and Ruthven (1988) determined diffusivities

in NaX with the Zero Length Column method. A very complete overview of available data of diffusion of hydrocarbons in zeolites can be found in the book of Ruthven and Kärger (1992).

Not much attention has however been paid to the adsorption and diffusion of isomers of heptane and octane and the higher carbon numbers paraffins. Moreover, most of the experiments were conducted at temperatures which are not relevant for catalytic conditions and deal with the adsorption or diffusion of single components. As all catalytic processes involve simultaneous adsorption and diffusion of product and reactant molecules, a knowledge of multicomponent rather than single component diffusion and adsorption properties is essential. Moore and Katzer (1972) and Satterfield and Cheng (1972) studied the counterdiffusion of liquid aromatic and naphthenic hydrocarbons in zeolite Y, but no data are available on the multicomponent adsorption and diffusion of paraffins in this adsorbent.

In processes like hydrocracking and hydroisomerization (Coonradt and Garwood, 1964; Martens et al., 1986), hydrocarbons are converted over a bifunctional catalyst. This is usually an acidic zeolite loaded with a well dispersed noble metal like Platinum or Palladium. In the present study, the effect of Platinum on the adsorption parameters of zeolite Y was determined and a comparison was made between the sodium and the acidic form of zeolite Y as well as between two samples with a different Si/Al-ratio. Adsorption constants and transport properties of paraffinic hydrocarbons and isomers with carbon numbers from 5 to 12 were determined using gas-solid chromatography at temperatures ranging from 275 to 400°C. Finally, competitive adsorption between paraffins was measured with perturbation chromatography.

Theoretical Aspects

Adsorption properties like equilibrium data and diffusivities are often measured with the chromatographic technique (Ruthven, 1984). Single component Henry constants and diffusion coefficients can be obtained by injecting a small pulse of this component in an inert carrier flowing through the bed of zeolite pellets and measuring the retention time and the peak broadening. This technique is often referred to as the pulse chromatographic method. In the perturbation chromatography technique used in this paper, the initial steady state in the column equilibrated with a given carrier mixture is perturbed by injecting a small amount of an adsorbing component at the inlet of the chromatographic column.

The equations used to extract the adsorption and diffusion parameters from the response of the system to a perturbation are given below.

Tracer Chromatography. An adsorbing component is injected in an inert carrier. The retention time of the injected component correlates to the adsorption parameters, whereas the peak broadening is caused by mass transfer resistances.

Assuming

- isothermal behavior
- constant velocity plug flow with axial dispersion
- flow pattern in external gas phase is described by Darcy's law (Coulson et al., 1991)
- the external film resistance is negligible
- adsorption occurs only in the micropores
- adsorption equilibrium is described by Henry's law
- mass transfer is described by a linear driving force (lumping micropore and macropore resistances).

the following expressions for the retention time and the peak broadening are obtained:

$$\mu = \frac{L}{v_f}[(\varepsilon_{ext} + \varepsilon_{macr}) + (1 - \varepsilon_{ext} + \varepsilon_{macr})RT\rho_c K_i'] \tag{1}$$

$$\frac{\sigma^2}{2\mu^2} = \frac{L}{v_f}\frac{(1 - \varepsilon_{ext} + \varepsilon_{macr})(RT\rho_c K_i')}{\mu^2} \times \left(\frac{r_c^2}{15D_{micr}} + \frac{R_p^2\left(1 + (RT\rho_c K_i')\left(\frac{1-\varepsilon_\mu}{\varepsilon_p}\right)\right)}{15D_{macr}}\right) + \frac{D_{ax}\varepsilon_{ext}}{v_f L} \tag{2}$$

The average superficial velocity v_f over the column is given by (Chiang et al., 1984):

$$v_f = v_{out}p_{out}\frac{3(p_{in} + p_{out})}{2\left(p_{in}^2 + p_{in}p_{out} + p_{out}^2\right)} \tag{3}$$

Perturbation Chromatography. Consider a column in which the carrier contains both an inert and an adsorbing component. This system, initially in equilibrium, is perturbed by a pulse of a second adsorbing component. Thus, we have a system with three components:

$i = 1$: the injected component, with $p_1 = p \cdot x_1$
$i = 2$: the adsorbing component of the carrier gas, with $p_2 = p \cdot x_2$
$i = 3$: the non adsorbing component of the carrier gas, with $p_3 = p \cdot x_3$.

Plug flow without axial dispersion and mass transfer limitations is assumed. The mass balances are written as:

$$v_f p \frac{\partial x_i}{\partial z} + (\varepsilon_{ext} + \varepsilon_{macr}) p \frac{\partial x_i}{\partial t} + (1 - \varepsilon_{ext} - \varepsilon_{macr}) \times \left(\frac{\partial q_i}{\partial t}\right) = 0 \qquad i = 1 \cdots 3 \tag{4}$$

These three equations are coupled through the continuity condition:

$$x_1 + x_2 + x_3 = 1 \tag{5}$$

The equilibrium adsorbed phase concentration q_i depends on the local concentration of all adsorbable components:

$$q_i = \varphi_i(p_1, p_2)\rho_{crys} RT \tag{6}$$

which for a multicomponent Langmuir adsorption isotherm yields:

$$\varphi_i = \frac{K_i' p x_i}{1 + L_1 p x_1 + L_2 p x_2} \tag{7}$$

After combining Eqs. (4), (6) and (7) and applying the chain rule:

$$\frac{dq_i}{dt} = \sum_j \frac{\partial q_i}{\partial x_j} \frac{\partial x_j}{\partial t} \tag{8}$$

one finds:

$$v_f \frac{\partial x_1}{\partial z} + (\varepsilon_{ext} + \varepsilon_{macr}) \frac{\partial x_1}{\partial t} + (1 - \varepsilon_{ext} - \varepsilon_{macr}) \times \left[\frac{K_1'(1 + L_2 p x_2)\rho_{crys} RT}{(1 + L_1 p x_1 + L_2 p x_2)^2}\right] \frac{\partial x_1}{\partial t} + (1 - \varepsilon_{ext} - \varepsilon_{macr}) \times \left[\frac{-K_1' x_1 L_2 p \rho_{crys} RT}{(1 + L_1 p x_1 + L_2 p x_2)^2}\right] \frac{\partial x_2}{\partial t} = 0 \tag{9}$$

$$v_f \frac{\partial x_2}{\partial z} + (\varepsilon_{ext} + \varepsilon_{macr}) \frac{\partial x_2}{\partial t} + (1 - \varepsilon_{ext} - \varepsilon_{macr}) \times \left[\frac{-K_2' x_2 L_1 p \rho_{crys} RT}{(1 + L_1 p x_1 + L_2 p x_2)^2}\right] \frac{\partial x_1}{\partial t} + (1 - \varepsilon_{ext} - \varepsilon_{macr}) \times \left[\frac{(1 + L_1 p x_1) K_2' \rho_{crys} RT}{(1 + L_1 p x_1 + L_2 p x_2)^2}\right] \frac{\partial x_2}{\partial t} = 0 \tag{10}$$

$$v_f \frac{\partial x_3}{\partial z} + (\varepsilon_{ext} + \varepsilon_{macr}) \frac{\partial x_3}{\partial t} = 0 \tag{11}$$

In this isothermal 3 component system, the response to a perturbation involves two mass transfer zones which propagate through the column with characteristic velocities determined by the multicomponent equilibrium isotherm. The mean retention time μ_i of these mass transfer zones is given by (see Appendix):

$$\mu_1 = \frac{L}{v_f}\left[(\varepsilon_{ext} + \varepsilon_{macr}) + (1 - \varepsilon_{ext} - \varepsilon_{macr}) \times \left(\frac{K_1' \rho_{crys} RT}{1 + L_2 p x_2}\right)\right] \tag{12}$$

$$\mu_2 = \frac{L}{v_f}\left[(\varepsilon_{ext} + \varepsilon_{macr}) + (1 - \varepsilon_{ext} - \varepsilon_{macr}) \times \left(\frac{K_2' \rho_{crys} RT}{(1 + L_2 p x_2)^2}\right)\right] \tag{13}$$

μ_2 also corresponds to the retention time of the response to a perturbation of the binary carrier with one of the components of that carrier. This expression allows the determination of the single component adsorption isotherm. By measuring at different partial pressures of the adsorbing component in the carrier gas, the complete isotherm can be obtained. The Henry and Langmuir adsorption constants are calculated from fitting of the experimental adsorption constants K_{exp}, defined as:

$$K_{exp} = \frac{K_1'}{1 + L_2 p x_2} \tag{14}$$

for μ_1 and

$$K_{exp} = \frac{K_2'}{(1 + L_2 p x_2)^2} \tag{15}$$

for μ_2, versus the partial pressure of the carrier gas adsorbing component. By injecting different types of molecules is the same carrier, differences in competition between the injected molecules and the carrier can be monitored.

Experimental

Four different zeolite samples were kindly provided by Prof. Johan Martens of the COK, KULeuven: zeolite NaY (from Zeocat) with a Si/Al ratio of 2.7, the same zeolite exchanged with 0.1 N NH_4Cl, another fraction of this NaY zeolite exchanged with an aqueous solution of $Pt(NH_3)_4Cl_2$ so as to contain 0.5 wt% Platinum, and finally a dealuminated USY zeolite with a Si/Al ratio

Table 1. Column and adsorbent properties.

	NaY	HY	Pt/NaY	USY
Column length (m)	0.255	0.265	0.262	0.36
Adsorbent mass (kg)	4.88×10^{-4}	5.11×10^{-4}	5.47×10^{-4}	6.7×10^{-4}
Bulk density (kg/m^3)	518	522	565	503
Dubinin surface area (m^2/g)	923	1004	918	882
Micropore volume (cc/g)	.328	.35	.326	.31
Crystal diameter (m)	9×10^{-7}	9×10^{-7}	9×10^{-7}	3.4×10^{-7}
Si/Al ratio	2.7	2.7	2.7	41

of 41. These zeolites were pelletized in a press by applying a pressure of about 200 bar. The pellet fraction from 250 to 400 μm was used to fill 1/8 in. diameter stainless steel columns with lengths of 0.25–0.4 m. The Platinum loaded zeolite was activated by rising the temperature to 400°C (at 6°C/min) with an oxygen flow. After a purge with nitrogen, a flow of hydrogen was passed over the catalyst for 1 h at 400°C to reduce the Platinum ions. The ammonium exchanged zeolite was activated by rising the temperature to 400°C at 6°C/min with a nitrogen flow and holding for 1 hour at this temperature.

The average crystal radius was determined by SEM and was 0.45 μm for the zeolites with Si/Al = 2.7 and 1.7 μm for zeolite NaY with Si/Al = 41. The micropore volume was determined by nitrogen adsorption (using a Fisons' Sorptomatic, 1990). Crystal densities were calculated theoretically, based on an ideal crystal structure. Column and adsorbent properties are given in Table 1. Before measurement, the temperature was raised at a rate of 5°C/min to 350°C and maintained at this temperature overnight.

The setup for the perturbation chromatography measurements is represented schematically in Fig. 1.

A mass flow controller (0–100 ml/min) regulates the flow rate of the hydrogen carrier gas. The pressure at the inlet of the column is monitored through a 10 bar pressure transducer. Before entering the chromatographic column, the hydrogen flow is passed through a reservoir filled with liquid hydrocarbon. The partial pressure of the hydrocarbon in the carrier flow can be adjusted by altering the temperature of the reservoir. The hydrogen/hydrocarbon equilibrium was calculated with the Redlich-Kwong-Soave model with Boston-Mathias modification. All hydrocarbons used were of spectrophotometric grade and purchased from ACROS.

The column with adsorbent is placed in a Varian 3300 GC-oven. Hydrocarbons are injected (typically

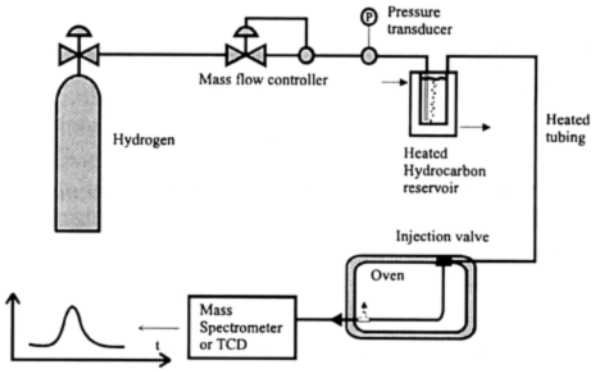

Figure 1. Experimental setup for the perturbation chromatography measurements.

0.1 μl) at the inlet of the column. The outlet of the column is at atmospheric pressure. After passing the column, the gas stream enters the detector, either a TCD (as a non specific detector), or a Balzer quadrupole mass spectrometer (QMG 112A), allowing individual components to be monitored and reaction products to be determined. For the measurements in the Henry domain, the hydrocarbon reservoir was removed from the setup. After subtraction of the baseline from the response curve, first and second moments were calculated by integration. The dead time of the system was determined at different flowrates and subtracted from the experimental retention time. Pressure drop over the column varied between one and two bar, gas flow rates between 1 and 6 Nml/s were used.

Results and Discussion

Henry Constants and Heats of Adsorption. Pulses of the different adsorbates were injected at the inlet of the column in an inert hydrogen flow. System linearity was

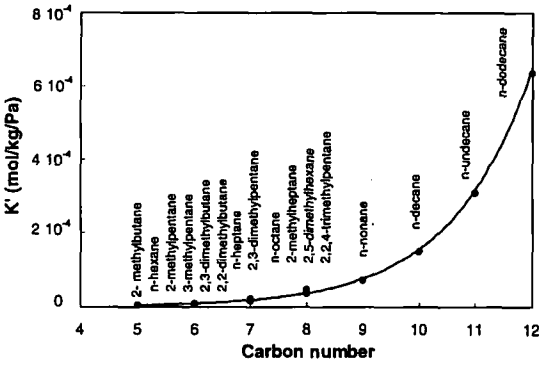

Figure 2. Henry constants of normal and branched paraffins on zeolite NaY (Si/Al 2.7) at 350°C.

confirmed by varying the injection volume. The Henry constants K' (calculated from the first moment of the response peak) of the linear and branched paraffins on zeolite NaY at 350°C are shown in Fig. 2.

An exponential increase of K' with the carbon number is observed. A similar exponential increase was also found by Hufton and Danner (1993) for adsorption of methane to *n*-butane on silicalite. The Henry constants of the isomers are somewhat higher than those of the linear chains (Table 2), but generally speaking it can be stated that the Henry adsorption constants are dependent on the molecular weight (number of carbon atoms) and not the molecular shape. This low effect of chain branching on the adsorption parameters is to be expected in a three dimensional pore system with large supercages. Experimental and modelling work delivered by Santilli and Zones (1990) showed that methyl and dimethyl branched isomers of n-hexane experience greater attractive interactions with the wall of the zeolite than the linear chain in zeolites with pores between 7 and 7.4 Å. This *inverse shape selectivity* is probably caused by a better steric fit of the branched hydrocarbons is the pore system. More hydrogen atoms have van der Waals interactions with the oxygen atoms of the framework, resulting in a stronger attraction. This is especially true for SSZ-24 and molecular sieves of the $AlPO_4$-5 family. However, Santilli (1986) didn't notice inverse shape selectivity for faujasites using the pore probe technique, but rather a preferential adsorption of the linear chains, whereas the present measurements indicate a stronger adsorption of the isomers. Moreover, it was shown that the Henry constants of the C8-paraffins increase with the degree of branching. A main difference between the pore probe technique and the chromatographic method, which could account for the observed disagreement, is that the pore probe technique is conducted with a mixed feed, whilst the present method invokes only one pure component at low loading. Further, Santilli's experiments concerned

Table 2. Henry constants of linear and branched chains at 300°C.

	K' (mol/kg/Pa)			
Sorbate	NaY	HY	Pt/Y	USY
2-methylbutane	8.2×10^{-6}	7.8×10^{-6}	1.0×10^{-5}	1.1×10^{-6}
n-hexane	1.9×10^{-5}	1.7×10^{-5}	2.3×10^{-5}	2.4×10^{-6}
2-methylpentane	2.0×10^{-5}	1.7×10^{-5}	2.4×10^{-5}	2.6×10^{-6}
3-methylpentane	2.0×10^{-5}	1.7×10^{-5}	2.4×10^{-5}	2.7×10^{-6}
2,3-dimethylbutane	2.0×10^{-5}	1.8×10^{-5}	2.4×10^{-5}	2.7×10^{-6}
2,2-dimethylbutane	2.1×10^{-5}	1.8×10^{-5}	2.4×10^{-5}	2.5×10^{-6}
n-heptane	4.4×10^{-5}	3.6×10^{-5}	5.4×10^{-5}	4.6×10^{-6}
2,3-dimethylpentane	5.1×10^{-5}	4.0×10^{-5}	6.1×10^{-5}	6.2×10^{-6}
n-octane	1.0×10^{-4}	7.9×10^{-5}	1.2×10^{-4}	8.3×10^{-6}
2-methylheptane	1.0×10^{-4}	7.9×10^{-5}	1.2×10^{-4}	8.6×10^{-6}
2,5-dimethylhexane	1.1×10^{-4}	8.3×10^{-5}	1.3×10^{-4}	1.1×10^{-5}
2,2,4-trimethylpentane	1.3×10^{-4}	9.1×10^{-5}	1.5×10^{-4}	9.5×10^{-6}
n-nonane	2.3×10^{-4}	1.7×10^{-4}	2.7×10^{-4}	1.5×10^{-5}
n-decane	5.3×10^{-4}	3.9×10^{-4}	5.4×10^{-4}	2.9×10^{-5}
n-undecane	1.2×10^{-3}	8.4×10^{-4}	—	5.7×10^{-5}
n-dodecane	2.7×10^{-3}	1.9×10^{-3}	—	1.1×10^{-4}

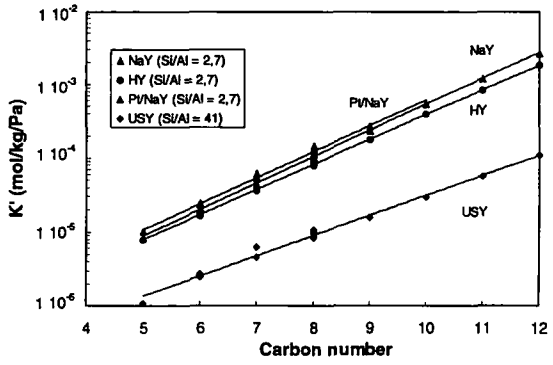

Figure 3. Henry constants of *n*-paraffins and isomers on NaY, HY, Pt/NaY and USY at 300°C.

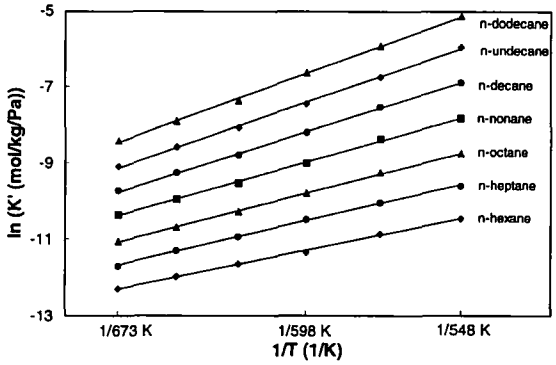

Figure 4. van 't Hoff plot for linear paraffins on zeolite NaY (Si/Al 2.7).

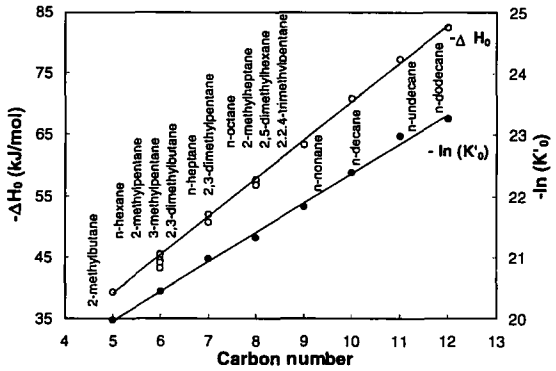

Figure 5. Limiting heats of adsorption and pre-exponential factors for zeolite NaY.

only hexane isomers, where it is clear now that the difference in adsorption properties between linear and branched chains becomes more important with rising chain length.

On comparing the data (Fig. 3) for four different zeolites NaY (Si/Al 2.7), Pt/NaY, HY and USY (Si/Al 41), one notices the same exponential trend for all the faujasite zeolites under investigation.

Due to a higher degree of dealumination, zeolite USY has a lower adsorption capacity than the other adsorbents. This effect becomes slightly more pronounced with rising chain length. Both a creation of mesopores and a loss of crystallinity as cation effects might be responsible for the reduction in adsorption capacity, but the loss of porosity due to mesopore formation remains rather low in this zeolite (Table 1).

The adsorption heats were calculated using the Henry constants in the temperature range from 275 to 400°C by linear regression (Fig. 4) of the van 't Hoff equation:

$$K' = K'_0 e^{\frac{-\Delta H_0}{RT}} \tag{16}$$

The van 't Hoff plots are linear over the whole temperature range. Resulting low coverage adsorption heats are shown in Fig. 5. A linear correspondence between carbon number and adsorption heat is found. For the faujasites with Si/Al 2.7, the adsorption heat increases with circa 6–7 kJ/mol per extra -CH_2- group for the linear chains. Within the experimental error, the isomers of hexane, heptane and octane have approximately the same adsorption heat as the unbranched chains (Table 3).

Experimental inaccuracy makes it rather difficult to observe differences in the heats of adsorption of normal and branched chains. On Pt/NaY, the measurements of the retention times were disturbed by conversion (alkane hydrogenolysis, dehydrogenation) of the alkanes on the Platinum, which probably explains the larger discrepancy between the adsorption heats of the branched and the unbranched chains on this zeolite.

The following expressions were extracted for zeolite NaY (Fig. 5):

$$-\Delta H_0 = 6.25CN + 7.91 \tag{17}$$

$$-\ln(K'_0) = 0.47CN + 17.6 \tag{18}$$

Introducing these two expressions into the van 't Hoff equation results in a general correlation for the Henry constants:

$$K' = \exp(-0.47CN - 17.6)e^{\frac{6.25CN+7.91}{RT}} \tag{19}$$

Danner and Hufton (1993) deduced a correlation of the same form for the adsorption of light normal

Table 3. Heats of adsorption at low coverage and pre-exponential factors sorbate. .

Sorbate	$-\Delta H_0$ (kJ/mol)				K_0' (mol/kg/Pa)			
	NaY	HY	Pt/Y	USY	NaY	HY	Pt/Y	USY
2-methylbutane	39.2	36.0	38.2	29.4	2.1×10^{-9}	3.4×10^{-9}	3.4×10^{-9}	2.7×10^{-9}
n-hexane	45.5	44.2	51.1	38.5	1.3×10^{-9}	1.4×10^{-9}	5.3×10^{-10}	8.8×10^{-10}
2-methylpentane	45.3	44.2	50.0	39.2	1.4×10^{-9}	1.3×10^{-9}	6.3×10^{-10}	7.8×10^{-10}
3-methylpentane	44.5	43.5	48.1	37.7	1.7×10^{-9}	1.6×10^{-9}	9.6×10^{-10}	1.2×10^{-9}
2,3-dimethylbutane	44.1	43.5	49.7	36.8	1.9×10^{-9}	1.6×10^{-9}	7.0×10^{-10}	1.4×10^{-9}
2,2-dimethylbutane	43.2	43.5	46.8	36.6	2.2×10^{-9}	1.6×10^{-9}	1.3×10^{-9}	1.7×10^{-9}
n-heptane	51.9	50.1	54.6	42.7	7.8×10^{-10}	8.7×10^{-10}	5.6×10^{-10}	6.6×10^{-10}
2,3-dimethylpentane	50.6	49.7	56.7	42.2	1.2×10^{-9}	1.0×10^{-9}	4.1×10^{-10}	6.2×10^{-10}
n-octane	57.5	56.0	59.9	49.9	5.5×10^{-10}	5.5×10^{-10}	4.0×10^{-10}	2.7×10^{-10}
2-methylheptane	57.2	55.7	57.4	48.0	6.0×10^{-10}	4.6×10^{-10}	6.5×10^{-10}	4.2×10^{-10}
2,5-dimethylhexane	57.1	56.0	60.4	47.8	6.3×10^{-10}	5.8×10^{-10}	4.0×10^{-10}	3.3×10^{-10}
2,2,4-trimethylpentane	56.8	54.5	66.4	47.6	8.4×10^{-10}	8.6×10^{-10}	1.2×10^{-10}	6.0×10^{-10}
n-nonane	63.4	62.0	67.6	54.0	3.3×10^{-10}	3.4×10^{-10}	1.7×10^{-10}	2.0×10^{-10}
n-decane	70.8	68.3	—	58.7	1.9×10^{-10}	2.0×10^{-10}	2.9×10^{-10}	1.4×10^{-10}
n-undecane	77.4	75.6	—	64.2	1.1×10^{-10}	9.7×10^{-11}	—	8.9×10^{-11}
n-dodecane	81.7	81.6	—	69.6	7.9×10^{-11}	6.1×10^{-11}	—	5.7×10^{-11}

alkanes on silicalite. They found an increase in adsorption heat of 9–10 kJ/mol per carbon atom. Atkinson and Curthoys (1981) measured a linear increase in adsorption heat for propane to pentane on NaY. Kiselev and Shcherbakova (1967) found a linear increase of the adsorption heat of normal paraffins on microporous silica gel up to C25. The adsorption heat of aromatics on NaY is not dependent on the molecular shape, but increases again linearly with the carbon number (Ruthven et al., 1993).

Jänchen and Stach (1985) measured a zero adsorption enthalpy of 81.6 kJ/mol for the adsorption of *n*-decane on NaY with Si/Al = 2.4 and 74.0 on NaY with Si/Al = 5. The present measurements yield a value of 70.8 kJ/mol for a Si/Al ratio of 2.7 and 57 for a Si/Al of 41 (Fig. 6). Dealumination thus results in a decrease in adsorption interaction energy, due to a reduction in polarization energy. Furthermore, the increase of adsorption heat with carbon number is lower (≈5 kJ/mol) for the dealuminated form of zeolite Y.

The heat of adsorption on NaY is 1–2 kJ/mol higher than on HY, as found by Atkinson and Curthoys (1981). Platinum dispersed in the zeolite pore system, even in a small fraction, leads to an increase of the adsorption heat, but has only a small influence on the variation of $-\Delta H_0$ with the carbon number.

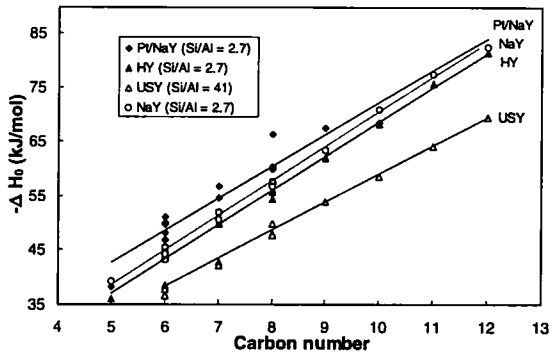

Figure 6. Limiting heats of adsorption of paraffins on zeolites NaY, HY, Pt/NaY and USY.

Diffusion Properties. Time constants for diffusion were calculated from the second moment of the chromatographic response curves. Peak broadening due to axial dispersion accounts for less then 5% of the overall peak broadening, whilst the injector and detector second order moment are less then 0.02 s^2 and can be neglected for these measurements. Apparent diffusional

Table 4. Transport properties in NaY at 300°C.

	K'_d	K' (mol/kg/Pa)	D_{mol} (m^2/s)	$K_d{}'D$ (m^2/s)	D_{macr} (m^2/s)
2-methylbutane	92.51	8.19×10^{-6}	5.75×10^{-5}	1.11×10^{-10}	3.86×10^{-6}
n-hexane	218.30	1.93×10^{-5}	5.07×10^{-5}	1.16×10^{-10}	3.78×10^{-6}
2-methylpentane	223.34	1.98×10^{-5}	5.10×10^{-4}	1.35×10^{-10}	4.39×10^{-6}
3-methylpentane	230.04	2.04×10^{-5}	5.20×10^{-5}	9.85×10^{-11}	3.21×10^{-6}
2,3-dimethylbutane	225.01	1.99×10^{-5}	5.24×10^{-5}	1.52×10^{-10}	4.96×10^{-6}
2,2-dimethylbutane	234.12	2.07×10^{-5}	5.26×10^{-5}	1.22×10^{-10}	3.98×10^{-6}
n-heptane	493.74	4.37×10^{-5}	4.70×10^{-5}	1.47×10^{-10}	4.76×10^{-6}
2,3-dimethylpentane	579.88	5.14×10^{-5}	4.85×10^{-5}	1.33×10^{-10}	4.31×10^{-6}
n-octane	1132.80	1.00×10^{-4}	4.36×10^{-5}	1.48×10^{-10}	4.79×10^{-6}
2-methylheptane	1161.89	1.03×10^{-4}	4.39×10^{-5}	1.06×10^{-10}	3.43×10^{-6}
2,5-dimethylhexane	1290.84	1.14×10^{-4}	4.45×10^{-5}	2.09×10^{-10}	6.75×10^{-6}
2,2,4-trimethylpentane	1462.20	1.30×10^{-4}	4.56×10^{-5}	1.33×10^{-10}	4.31×10^{-6}
n-nonane	2607.45	2.31×10^{-4}	4.10×10^{-5}	1.97×10^{-10}	6.36×10^{-6}
n-decane	6045.68	5.35×10^{-4}	3.83×10^{-5}	7.56×10^{-11}	2.44×10^{-6}
n-undecane	13557.02	1.20×10^{-3}	3.63×10^{-5}	1.47×10^{-10}	4.76×10^{-6}
n-dodecane	30260.22	2.68×10^{-3}	3.43×10^{-5}	1.91×10^{-10}	6.17×10^{-6}

activation energies, defined as:

$$D = D_0 e^{(-E_D/RT)} \tag{20}$$

increase linearly with the chain length and are of the same magnitude as the heats of adsorption. Moreover, the product of the Henry adsorption coefficients and the apparent diffusion coefficient is a constant for all paraffins and all zeolites under study. This points at macropore diffusion control, which means that transport of paraffins in the zeolite pellets is not limited by micropore diffusion. This is not unexpected for strongly adsorbing substances in crystals of 0.9 μm diameter, packed in pellets of 250–400 μm diameter. Hsu et al. (1981) measured diffusivities of *n*-butane and *n*-hexane in NaY over the range from 105°C to 240°C with the chromatographic technique and concluded that the intracrystalline diffusion was too rapid to be detected. This seems also to be true for the present measurements.

Macropore diffusion coefficients were calculated following Eq. (5), assuming a mean pellet diameter of 325 μm (Table 4). The calculated effective macropore diffusion coefficients are about a factor 10 lower then the molecular diffusion coefficients. When macropore diffusion occurs by molecular diffusion, the effective macropore diffusion coefficient correlates to the molecular diffusion coefficient as:

$$D_{macr} = \frac{D_{mol}\varepsilon_{pel}}{\tau} \tag{21}$$

With typical values of 0.3 for ε_{pel} and 3 for the tortuosity (Ruthven and Kärger, 1992), the effective macropore diffusivity equals the molecular diffusivity divided by 10. This agreement between the measurements and macropore diffusion model provides evidence that the slowest step in mass transfer in this system (which is similar to that used in many catalytic experiments) is governed by hindered molecular diffusion in the macropores of the pellets.

A model including axial dispersion, mass transfer through the pellets and adsorption in the micropores was solved numerically in order to verify the validity of the model and the parameter extraction by the method of moments. A linear driving force for diffusion in the pellets was assumed. The time domain partial differential equations were transformed into ordinary differential equations by orthogonal collocation. The method of backward difference formulas was used for the time integration.

In Fig. 7, a comparison is made between the experimental chromatograms and the calculated response. The transport and adsorption parameters which were found by the method of moments were used in

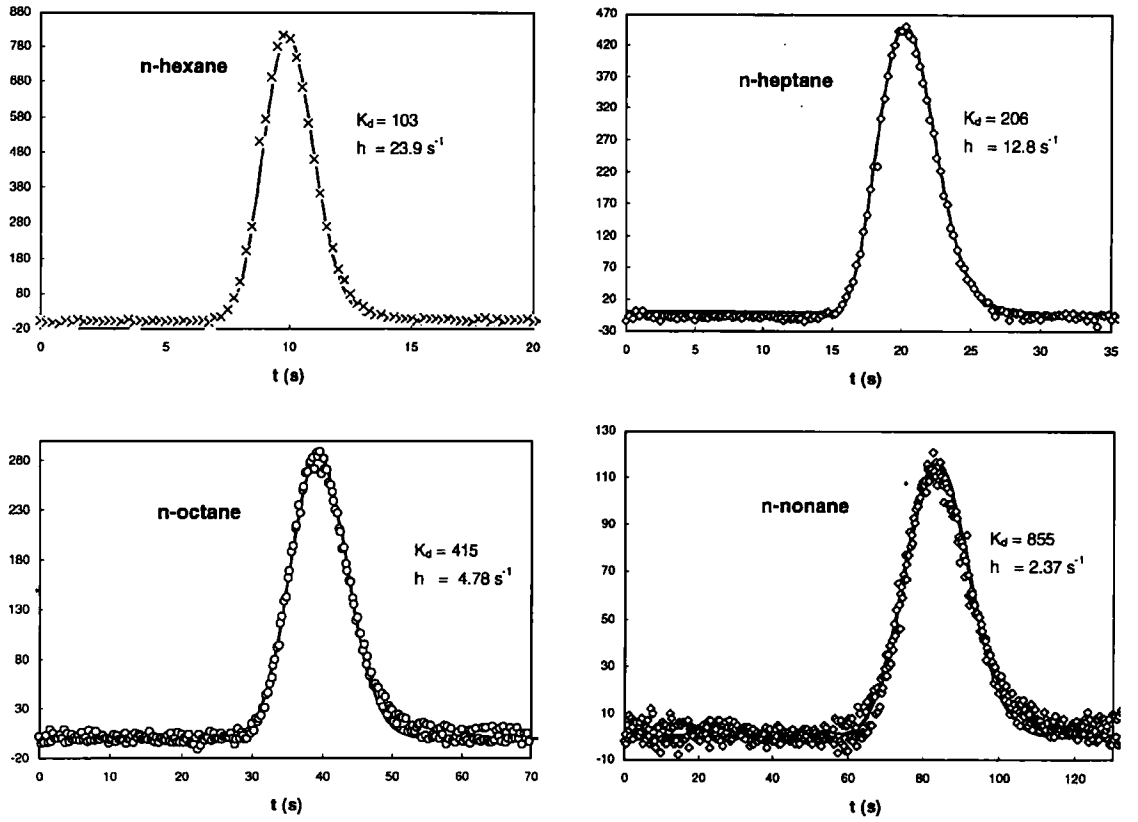

Figure 7. Experimental and theoretical response curves for NaY (Si/Al 2.7) at 350°C.

these simulations. Satisfying agreement between the calculated and experimental curves is found, which means that the method of moments provides reliable results, and that the linear driving force model is a good approximation for interpretation of the response curves.

Pure and Multicomponent Adsorption Isotherms. Low pressure equilibrium isotherms of *n*-octane, *n*-decane and *n*-dodecane on zeolite NaY with a Si/Al ratio 2.7 were measured using perturbation chromatography. In a first set of experiments, a hydrogen flow saturated with one of the *n*-paraffins in equilibrium with the adsorbent, was perturbed by injecting a pulse of this paraffin at the inlet of the column. The response to this perturbation involves one mass transfer zone, of which the mean retention time correlates to the local slope of the equilibrium isotherm. Figure 8 shows the response to a perturbation of a mixed *n*-octane/hydrogen flow by different *n*-paraffins. A non specific TCD detector was used to record this chromatographic response.

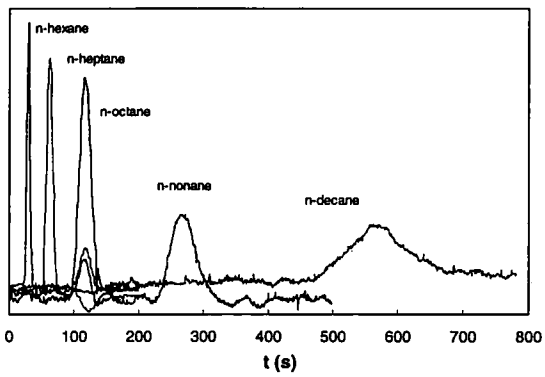

Figure 8. Chromatographic response to a perturbation of a mixed *n*-octane/hydrogen feed (mol fraction *n*-octane in feed: 0.014; adsorbent: NaY (Si/Al 2.7); T = 325°C; p_{col} = 1.17 bar).

When *n*-octane is injected, only one peak is observed, whereas two peaks are observed if a component different from the one in the carrier is injected. One of these two peaks corresponds to the single peak obtained after injecting *n*-octane. Furthermore, the retention

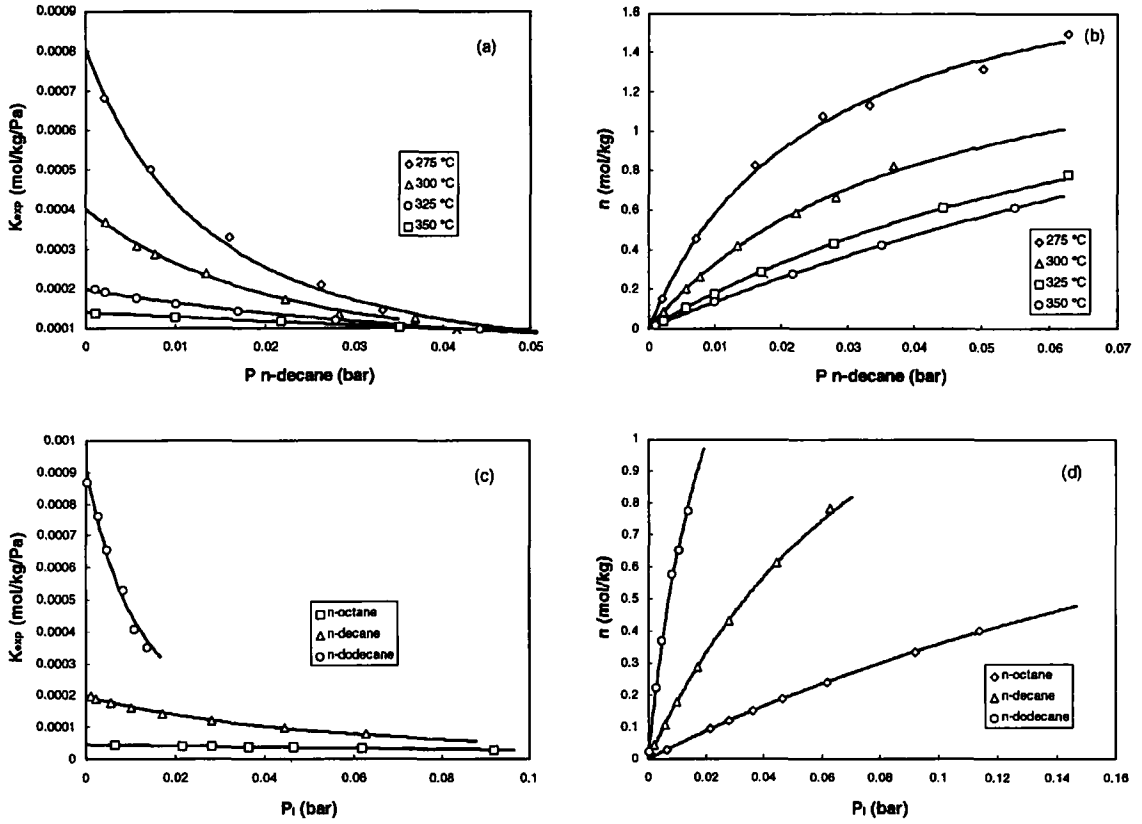

Figure 9. Equilibrium isotherms of *n*-paraffins on NAY (Si/Al 2.7). Experimental and fitted adsorption constants (a) and isotherms (b) of *n*-decane; experimental adsorption constants (c) and isotherms (d) at 325°C ($p_{col} = 1.18$ bar).

time of a hydrogen perturbation equals that of *n*-octane, as predicted by theory.

Experiments were conducted with rising mole fractions of hydrocarbon in the feed. An upper limit to the concentration of hydrocarbons is set by detector limitations. At too high paraffin/hydrogen ratios, the mass transfer zone cannot be measured due to a high background signal. As a consequence, only partial equilibrium isotherms can be obtained. Increasing the injection volume to increase the detection limit violates the assumption that the mole fraction of the injected component is negligible. Maximum mole fractions of circa 0.1 were used, corresponding to a partial pressure of 0.1 bar.

The experimental adsorption constants were fitted to the model using a quasi-Newton fitting algorithm (Harwell Subroutine Library, 1973). Experimental and fitted isotherms of *n*-octane, *n*-decane and *n*-dodecane at 325°C, as well as *n*-decane isotherms at a range of temperatures are shown in Fig. 9. From this figure, it is clear that the longer chains adsorb better than the shorter chains, as shown before. In the covered pressure range, a factor 4 in adsorption capacity between *n*-octane and *n*-decane or *n*-decane and *n*-dodecane at a constant pressure is observed. Table 5 gives the fitted Henry and Langmuir adsorption parameters. The maximum adsorption capacities were calculated from the experimental isotherms at 325°C using:

$$n_s = \frac{K'}{L} \tag{22}$$

Table 5. Henry and Langmuir constants of *n*-paraffins on NaY at 325°C.

Sorbate	K' (mol/kg/bar)	L (l/bar)	K'/L (mol/kg)*	$n_s^\dagger$
n-octane	4.57	2.7	1.69	2.01
n-decane	19.8	9.8	2.02	1.69
n-dodecane	90.9	41.5	2.19	1.44

*Adsorption capacity estimated from the experimental isotherm.
†Adsorption capacity estimated from the liquid density and the micropore volume.

Table 5 also gives the adsorption capacities estimated from the micropore volume and the liquid densities of the paraffins at room temperature, which decrease from 2 mol/kg for *n*-octane to 1.44 mol/kg for *n*-dodecane. However, the experimental capacities (Eq. (22)) increase from 1.7 for *n*-octane to 2.2 for *n*-dodecane. This is not unexpected as only the lower partial pressure range is accessible by the perturbation method and Langmuir behaviour is assumed over the full range. Measurements with other techniques at higher coverage will probably require another isotherm equation. Nevertheless, the experimental values for the capacities are acceptable. Temperature dependence of the *n*-decane Langmuir adsorption constants is depicted in Table 6. The Langmuir adsorption heat of *n*-decane amounts 81.7 kJ/mol, the heat of adsorption at low coverage equals 70.8 kJ/mol. Taking experimental errors into account, one might conclude that the capacity n_s is independent of the temperature. Results of perturbation experiments in

Table 6. Langmuir constants of *n*-decane on NaY.

T (°C)	L (1/bar)
275	38.9
300	23.3
325	9.8
350	4.7

which an hydrogen/*n*-decane carrier was perturbed with a pulse of a second normal paraffin are shown in Fig. 10.

Even at higher loadings, competition between higher and lower molecular weight *n*-paraffins is observed. From this type of measurements, multicomponent Langmuir constants of the adsorbing carrier component can be determined. Experimental isotherms with *n*-decane, *n*-dodecane (Fig. 11) and *n*-octane in hydrogen as carrier at 325°C were used to calculate the Langmuir constants. These multicomponent

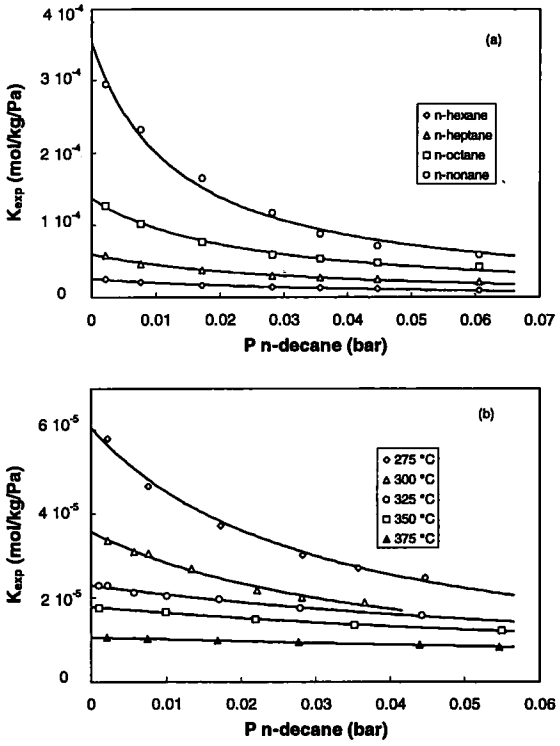

Figure 10. (a) Binary adsorption constants (experimental and fitted) of *n*-hexane, *n*-heptane, *n*-octane and *n*-nonane with *n*-decane/hydrogen as carrier at 275°C. (b) Temperature dependence of *n*-heptane adsorption with *n*-decane/hydrogen as carrier ($p_{col} = 1.16$) bar.

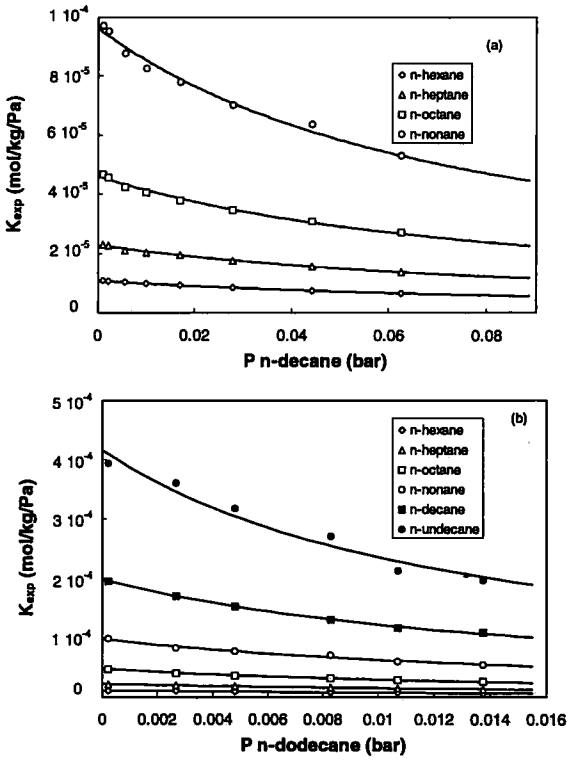

Figure 11. Binary adsorption constants of *n*-paraffins at 325°C on zeolite NaY. (a) carrier: *n*-decane/hydrogen ($p_{col} = 1.17$ bar) (b) carrier: *n*-dodecane/hydrogen ($p_{col} = 1.2$) bar.

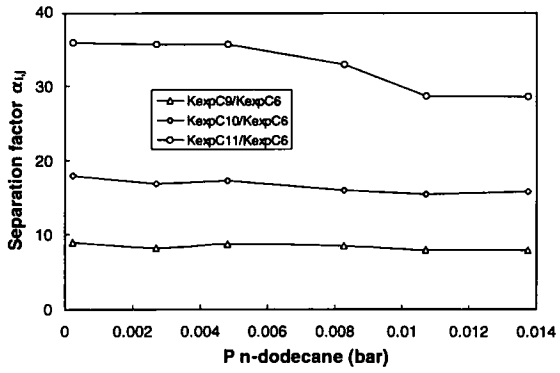

Figure 12. Separation factors of n-paraffins on NaY at 325°C.

Langmuir constants are approximately the same as the pure isotherm Langmuir constants (Table 5), and show the same increase with chain length as the Henry constants.

Separation factors, defined as:

$$\alpha_{i,j} = \frac{K_{\text{exp},i}}{K_{\text{exp},j}} \tag{23}$$

are plotted in Fig. 12 as a function of total pressure, which is also the partial pressure of the adsorbing carrier gas. The Langmuir model suggests a constant separation factor over the whole pressure range. It is noted that the separation factor tends to decrease at higher loadings, implying that the multicomponent adsorption behaviour deviates from the multicomponent Langmuir equation. Nevertheless, this deviation remains rather limited, so that the extended Langmuir isotherm might still be used to describe the competitive adsorption between n-paraffins on zeolite Y, at least for use in kinetic models for certain multicomponent reactions with hydrocarbons, such as for example hydrocracking or catalytic cracking.

Conclusion

Chromatographic measurements revealed strong differences in adsorption properties of linear paraffins, as a function of chain length, on zeolite Y. Henry and Langmuir constants increase with a factor two per extra carbon group. The influence of chain branching on adsorption and macropore diffusion remains limited. The adsorption properties show the same tendencies for zeolites NaY, HY, Pt/NaY and USY. Perturbation chromatography allowed the study of competitive adsorption between paraffins of different chain length. A strong competition between longer and shorter paraffins is observed, which can be adequately described by a multicomponent Langmuir adsorption isotherm. More accurate description of multicomponent equilibria requires measurements in the high coverage area and this is not possible with the present technique. Methods such as gravimetry and isotope tracer chromatography will be used in the near future to study the competitive adsorption at high coverage.

The knowledge of the multicomponent adsorption equilibrium of paraffins on the zeolite catalysts is useful in getting a better understanding of selectivity effects in multicomponent reactions. For example, the selective hydroconversion of the longer paraffin of a mixed paraffin feed, as mentioned by Dauns and Weitkamp (1986), can easily be understood in terms of competitive adsorption. Since longer paraffins are more strongly adsorbed, their internal concentration in the pores of the zeolite catalyst is higher than that of the shorter chains. As a consequence, longer paraffins are converted to a higher extent than the (less strongly adsorbed) shorter chains, explaining the selective conversion of the longer hydrocarbon chains. Kinetic investigations and modelling are under way in order to test this hypothesis.

Appendix

The characteristic shock velocities w_i of the mass transfer zones propagating through the column are found by casting the differential Eqs. (9), (10) and (11) into matrix form, and calculating the eigenvalues λ of the coefficient matrix:

$$\frac{1}{v_f}\begin{vmatrix} A + B\left[\frac{K_1'(1+L_2px_2)\rho_{crys}RT}{(1+L_1px_1+L_2px_2)^2}\right] - \lambda v_f & \frac{B(-K_1'x_1L_2p\rho_{crys}RT)}{(1+L_1px_1+L_2px_2)^2} & 0 \\ \frac{B(-K_2'x_2L_1p\rho_{crys}RT)}{(1+L_1px_1+L_2px_2)^2} & A + B\left[\frac{K_2'(1+L_1px_1)\rho_{crys}RT}{(1+L_1px_1+L_2px_2)^2}\right] - \lambda v_f & 0 \\ 0 & 0 & A + B\varepsilon_{micr} - \lambda v_f \end{vmatrix} = 0 \tag{A1}$$

with:

$$A = \varepsilon_{ext} + \varepsilon_{macr} \quad \text{and} \quad B = 1 - (\varepsilon_{ext} + \varepsilon_{macr}) \quad \text{(A2)}$$

The above matrix has three roots, corresponding to the three eigenvalues of the matrix. The first eigenvalue λ_1 is given by:

$$\lambda_1 = \frac{(\varepsilon_{ext} + \varepsilon_{macr}) + (1 - \varepsilon_{ext} - \varepsilon_{macr})\varepsilon_{micr}}{v_f} \quad \text{(A3)}$$

The propagation velocity of the first physically possible shock to occur is thus given by:

$$w_1 = \frac{v_f}{(\varepsilon_{ext} + \varepsilon_{macr}) + (1 - \varepsilon_{ext} - \varepsilon_{macr})\varepsilon_{micr}} \quad \text{(A4)}$$

This corresponds with the flow of the carrier. The two other eigenvalues are found by solving the equation:

$$\frac{1}{v_f}\left[\left(\left(A + B\left(\frac{K_1'(1 + L_2 p x_2)\rho RT}{Z^2}\right)\right) - \lambda v_f\right) \times \left(\left(A + B\left(\frac{K_2'(1 + L_1 p x_1)\rho RT}{Z^2}\right)\right) - \lambda v_f\right) - \frac{B^2(\rho RT)^2 K_1' K_2' L_1 L_2 x_1 x_2 p^2}{Z^4}\right] = 0 \quad \text{(A5)}$$

with:

$$Z = 1 + L_1 p x_1 + L_2 p x_2 \quad \text{(A6)}$$

Put:

$$A + B\left(\frac{K_1'(1 + L_2 p x_2)\rho RT}{Z^2}\right) = \alpha \quad \text{(A7)}$$

$$A + B\left(\frac{K_2'(1 + L_1 p x_1)\rho RT}{Z^2}\right) = \beta \quad \text{(A8)}$$

$$\frac{B^2(\rho RT)^2 K_1' K_2' L_1 L_2 x_1 x_2 p^2}{Z^4} = \gamma \quad \text{(A9)}$$

So Eq. (A5) can be written as:

$$\lambda^2 v_f^2 - (\alpha + \beta)\lambda v_f + (\alpha\beta - \gamma) = 0 \quad \text{(A10)}$$

Since x_1 is the mole fraction of the injected component in the external gas phase and in the macropores, it is assumed that x_1 is negligible small. From this, the γ term can be cancelled in Eq. (A10) and the following roots are found:

$$\lambda_2 v_f = \frac{\alpha + \beta + \sqrt{(\alpha - \beta)^2}}{2} = \alpha = A + B\left(\frac{K_1'(1 + L_2 p x_2)\rho RT}{(1 + L_1 p x_1 + L_2 p x_2)^2}\right) \quad \text{(A11)}$$

$$\lambda_3 v_f = \frac{\alpha + \beta - \sqrt{(\alpha - \beta)^2}}{2} = \beta = A + B\left(\frac{K_2'(1 + L_1 p x_1)\rho RT}{(1 + L_1 p x_1 + L_2 p x_2)^2}\right) \quad \text{(A12)}$$

Since x_1 is small (injected component), these Eqs. (A12) and (A13) can be reduced to:

$$\lambda_2 = \frac{1}{v_f}\left(A + B\left(\frac{K_1'\rho RT}{(1 + L_2 p x_2)}\right)\right) \quad \text{(A13)}$$

$$\lambda_3 = \frac{1}{v_f}\left(A + B\left(\frac{K_2'\rho RT}{(1 + L_2 p x_2)^2}\right)\right) \quad \text{(A14)}$$

corresponding with two distinct wave propagation velocities w_2 and w_3:

$$w_2 = \frac{v_f}{(\varepsilon_{ext} + \varepsilon_{macr}) + (1 - \varepsilon_{ext} - \varepsilon_{macr})\left[\frac{K_1'\rho_{crys}RT}{(1 + L_2 p x_2)} + \varepsilon_{micr}\right]} \quad \text{(A15)}$$

$$w_3 = \frac{v_f}{(\varepsilon_{ext} + \varepsilon_{macr}) + (1 - \varepsilon_{ext} - \varepsilon_{macr})\left[\frac{K_2'\rho_{crys}RT}{(1 + L_2 p x_2)^2} + \varepsilon_{micr}\right]} \quad \text{(A16)}$$

The retention times of the perturbations are given by $\mu_i = L/w_i$:

$$\mu_1 = \frac{L}{v_f}\left[(\varepsilon_{ext} + \varepsilon_{macr}) + (1 - \varepsilon_{ext} - \varepsilon_{macr}) \times \left(\varepsilon_{micr} + \frac{K_1'\rho_{crys}RT}{1 + L_2 p x_2}\right)\right] \quad \text{(A17)}$$

$$\mu_2 = \frac{L}{v_f}\left[(\varepsilon_{ext} + \varepsilon_{macr}) + (1 - \varepsilon_{ext} - \varepsilon_{macr}) \times \left(\varepsilon_{micr}\frac{K_2'\rho_{crys}RT}{(1 + L_2 p x_2)^2}\right)\right] \quad \text{(A18)}$$

Nomenclature

D_{micr}	Micropore diffusion coefficient	m^2/s
D_{macr}	Macropore diffusion coefficient	m^2/s
D_{mol}	Molecular diffusion coefficient	m^2/s

D_{ax}	Axial dispersion coefficient	m^2/s
h	Mass transfer coefficient	s^{-1}
K_{exp}	Experimental adsorption value	mol/(kg.Pa)
K_i'	Henry constant of component i	mol/(kg.Pa)
K_d	Dimensionless adsorption constant	—
L	Column length	m
L_i	Langmuir constant of component i	Pa^{-1}
n_i	Amount adsorbed in the solid	mol/kg
n_s	Maximal adsorption capacity	mol/kg
p	Total pressure	Pa
p_{col}	Mean total column pressure	Pa
p_i	Partial pressure of component i	Pa
p_{in}	Column inlet pressure	Pa
p_{out}	Column outlet pressure	Pa
q_i	Amount of component i in the micropores	Pa
r_c	Mean crystal radius	m
R_p	Mean pellet radius	m
R	Ideal gas constant	J/(mol.K)
t	Time	s
T	Temperature	K
v_f	Superficial velocity in adsorbent column	m/s
v_{out}	Velocity at the outlet of the column	m/s
w_i	Wave propagation velocity	m/s
x_i	Molar fraction of component i	—
z	Axial position	—

Greek letters

$\alpha_{i,j}$	Separation factor	—
ΔH_0	Heat of adsorption	kJ/mol
ε_{ext}	Bed voidage, external porosity	—
ε_{macr}	Macropore porosity	—
ε_{micr}	Micropore porosity	—
ε_p	Pellet porosity	—
φ	Adsorption isotherm form	
μ	Peak retention time	s
ρ_c	Crystal density	kg/m^3
σ^2	Variance of the peak	s^2
τ	Tortuosity factor	—

Acknowledgments

This research is supported by an IWT scholarship (J.D.), IUAPII-16 (G.B.) and a Grant of the NFWO (G.B. 9.0231.95). Constructive discussions with Professor J.A. Martens of the KULeuven are acknowledged.

References

Atkinson, D. and G. Curthoys, "Heats and Entropies of Adsorption of Saturated Hydrocarbons by Zeolites X and Y," *J. Chem. Soc., Faraday Trans. I.*, **77**, 897–907 (1981).

Bolton, A.P., "Hydrocracking, Isomerization, and Other Industrial Processes," *ACS Monogr.*, **171**, 714–779 (1976).

Burgess, C.G.V., R.H.E. Duffett, G.J. Minkoff, and R.G. Taylor, "Sorption of Long Chain Normal Paraffins in Molecular Sieves," *J. Appl. Chem.*, **14**, 350–360 (1964).

Chiang, A.S., A.G. Dixon, and Y.H. Ma, *Chem. Eng. Sci.*, **39**, 1451 (1984).

Coonradt, H.L. and W.E. Garwood, *Mechanism of Hydrocracking., I&EC Process Design and Development*, **1**, 38–45 (1964).

Coulson, J.M., J.F. Richardson, J.R. Backhurst, and J.H. Harker, *Chemical Engineering*, vol. 2, p. 133, Pergamon Press, 1991.

Dauns, H. and J. Weitkamp, "Modelluntersuchungen Zum Isomerisieren und Hydrocracken Von Alkan-Gemischen an Einem Pd/LaY-Zeolith-Katalysator," *Chem.-Ing.-Tech.*, **11**, 900–902 (1986).

Eic, M. and D.M. Ruthven, "Diffusion of Linear Paraffins and Cyclohexane in NaX and 5A Zeolite Crystals," *Zeolites*, **8**, 472–479 (1988).

Eic, M., M. Goddard, and D.M. Ruthven, "Diffusion of Benzene in NaX and Natural Faujasite," *Zeolites*, **8**, 327–331 (1988).

Harlfinger, R., D. Hoppach, U. Quaschik, and K. Quitzsch, "Adsorption of C_4 Hydrocarbons on X-Zeolites Containing Li^+, Na^+, K^+, Rb^+ and Cs^+ Cations," *Zeolites*, **3**, 123–128 (1983).

Harwell Subroutine Library, *AERE*, Harwell, Berkshire, 1973.

Hrúzik, D., J. Krupcík, and P.A. Leclercq, "Determination of Adsorption Isotherms for 1-Heptene Adsorbed on Synthetic NaX- and NaY-Zeolites from *n*-Heptane Solutions," *Zeolites*, **10**, 213–215 (1990).

Hsu, L.-K., P. Hsu, and H.W. Haynes, Jr., "Effective Diffusity by the Gas Chromatography Technique: Analysis and Application to Measurements of Diffusion of Various Hydrocarbons in Zeolite NaY," *AIChE Journal*, **27**(1), 81–91 (1981).

Hufton, J.R. and R.P. Danner, "Gas-Solid Diffusion and Equilibrium Parameters by Tracer Pulse Chromatography," *Chem. Eng. Sci.*, **46**(8), 2079–2091 (1991).

Hufton, J.R. and R.P. Danner, "Chromatographic Study of Alkanes in Silicalite: Equilibrium Properties," *AIChE Journal*, **39**(6), 954–961 (1993)

Hulme, R., R.E. Rosenweig, and D.M. Ruthven, "Binary and Ternary Equilibria for C_8 Aromatics on K-Y Faujasite," *Ind. Eng. Res.*, **30**, 752–760 (1991).

Jänchen, J. and H. Stach, "Dependence of the Adsorption Equilibrium of *n*-Decane on the Si/Al-Ratio of Faujasite Zeolites," *Zeolites*, **5**, 57–59 (1985).

Kärger, J. and D.M. Ruthven, *Diffusion in Zeolites*, pp. 434–445, John Wiley and Sons, 1992.

Kärger, J., H. Pfeifer, M. Rauscher, and A. Walter, "Self-Diffusion of *n*-paraffins in NaX Zeolite," *J.C.S. Faraday*, **76**, 717–737 (1980).

Kiselev, A.V. and K.D. Shcherbakova, *Proceedings of the 1st Zeolite Conference*, London, p. 289, 1967.

Martens, J.A., P.A. Jacobs, and J. Weitkamp, "Attemps to Rationalize the Distributions of Hydrocracked Products. I. Qualitative Description of the Primary Hydrocracking Modes of Long Chain Paraffins in Open Zeolites," *Applied Catalysis*, **20**, 239–281 (1986).

Moore, R.M. and J.R. Katzer, "Counterdiffusion of Liquid Hydrocarbons in Type Y Zeolite: Effect of Molecular Size, Molecular Type, and Direction of Diffusion," *AIChE J.*, **4**, 816–824 (1972).

Ruthven, D.M., *Principles of Adsorption and Adsorption Processes*, John Wiley and Sons, Canada, 1984.

Ruthven, D.M. and M. Goddard, "Sorption and Diffusion of C_8 Aromatic Hydrocarbons in Faujasite Type Zeolites. I. Equilibrium Isotherms and Separation Factors," *Zeolites*, **6**, 275–282 (1986).

Ruthven, D.M. and M. Goddard, "Sorption and Diffusion of C_8 Aromatic Hydrocarbons in Faujasite Type Zeolites. II. Sorption Kinetics and Intracrystalline Diffusities," *Zeolites*, **6**, 283–289 (1986).

Ruthven, D.M. and B.K. Kaul, "Adsorption and Diffusion of Aromatics in NaX Zeolite," *AIChE Annual Meeting*, St. Louis, 1993.

Santilli, D.S., "Pore Probe: A New Technique for Measuring the Concentrations of Molecules Inside Porous Materials at Elevated Temperatures," *Journal of Catalysis*, **99**, 335–341 (1986).

Santilli, D.S. and S.I. Zones, "Secondary Shape Selectivity in Zeolite Catalysis," *Catalysis Letters*, **7**, 383–388 (1990).

Satterfield, C.N. and C.S. Cheng, "Liquid Counterdiffusion of Selected Aromatic and Naphthenic Hydrocarbons in Type Y Zeolites," *AIChE J.*, **4**, 724–728 (1972).

Stach, H., U. Lohse, H. Thamm, and W. Schirmer, "Adsorption Equilibria of Hydrocarbons on Highly Dealuminated Zeolites," *Zeolites*, **6**, 74–90 (1986).

Thamm, H., H. Stach, and W. Fiebig, "Calorimetric Study of the Absorption of *n*-Butane and But-I-ene on a Highly Dealuminated Y-Type Zeolite and on Silicalite," *Zeolites*, **3**, 94–97 (1983).

Ward, J.W., "Hydrocracking Processes and Catalysts," *Fuel Processing Technology*, **35**, 55–85 (1993).